Diffraction

G. Roth

This document has been published in

Thomas Brückel, Gernot Heger, Dieter Richter, Georg Roth and Reiner Zorn (Eds.): Lectures of the JCNS Laboratory Course held at Forschungszentrum Jülich and the research reactor FRM II of TU Munich
In cooperation with RWTH Aachen and University of Münster
Schriften des Forschungszentrums Jülich / Reihe Schlüsseltechnologien / Key Technologies, Vol. 39
JCNS, RWTH Aachen, University of Münster
Forschungszentrum Jülich GmbH, 52425 Jülich, Germany, 2012
ISBN: 978-3-89336-789-4

4 Diffraction

G. Roth
Institute of Crystallography
RWTH Aachen University

Contents

Lecture Notes of the JCNS Laboratory Course Neutron Scattering

4.1 Introduction

Each scattering experiment performed with any type of radiation - regardless of whether it involves massive particles like neutrons and electrons or electromagnetic waves like x-rays or visible light - has a total of four attributes which altogether characterize the type of the scattering experiment as well as the information that can be obtained from such an experiment. These attributes and their characteristics are:

Elastic scattering, which involves the conservation of the energy of the particle or quantum during the scattering process, *inelastic* scattering, corresponding to a loss or gain of particle or quantum energy during the scattering event, *coherent* scattering which involves the interference of waves (recall that, according to the particle-wave dualism first stated by de Broglie (1924), each particle may also be described by wave which can interfere with other particle waves) and finally *incoherent* scattering which is scattering without interference.

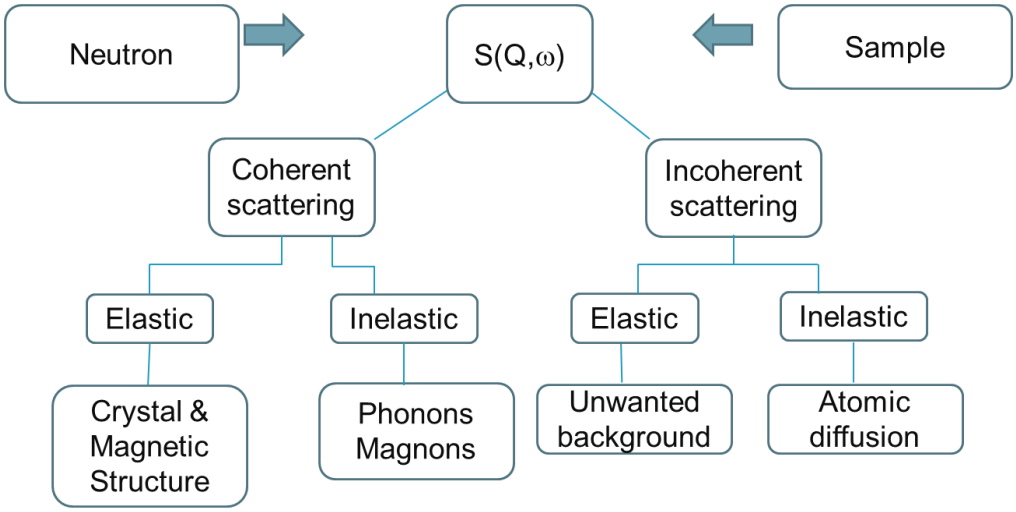

Fig. 4.1: Scattering function S(Q,ω) of a general scattering experiment (Q: scattering vector, ω: frequency), its different contributions and information that can be obtained from them.

This chapter will deal mostly with neutron *diffraction* which is, in the above nomenclature of a general scattering experiment, equivalent to *elastic coherent scattering* of neutrons.

Most of the readers of this chapter will be more or less familiar with x-ray diffraction from crystals, which has been demonstrated for the first time by Laue in 1912 and, since then, has developed into the most powerful method for obtaining structural information on crystalline materials. Diffraction - in sharp contrast to imaging techniques like optical or electron microscopy - has no principal limitation as to the spatial resolution, expressed in units of the wavelength of the radiation used for diffraction or imaging: While the resolution of imaging is limited to half the wavelength (recall the Abbe diffraction limit) diffraction can yield useful information, for instance, on bond distances between atoms on a length scale that is by two to three orders of magnitude smaller than the wavelength. On the other hand, diffraction, other than imaging,

requires 3-dimensional periodicity that is underlying the concept of the crystalline state (see chapter 3, symmetry in crystals).

This chapter will discuss the basics and peculiarities of neutron diffraction from either single- or polycrystalline matter. We will start by discussing scattering of neutrons from individual atoms, then turn to the geometry of diffraction from crystals, treat the subject of diffraction intensities and end with a discussion of a few experimental issues connected to the instruments which will be used in the practical part of the course. Examples of applications of these methods will be given in chapter 8 "structural analysis". The subject of magnetic neutron diffraction and scattering will be discussed separately in chapter 7.

4.2 Neutron waves & neutron scattering

The three major probes for investigating condensed matter are photons, electrons and neutrons. While photons are the (massless) quanta of electromagnetic radiation (e.g. x-rays, including synchrotron radiation, but also visible light, gamma-rays etc.) electrons and neutrons are massive particles. Owing to the wave-particle-duality, a central concept of quantum mechanics that states that all particles exhibit both wave- and particle-properties, the formal description of a scattering experiment does not differ for these different probes. However, the relation between energy and wavelength of the probes and also the mechanisms by which they interact with matter are vastly different.

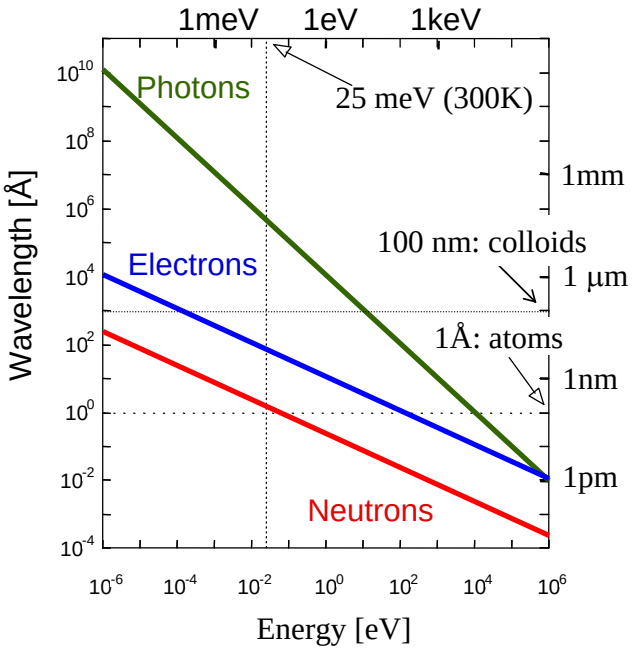

Fig. 4.2: *Comparison of the three probes - neutrons, electrons and photons - in a double logarithmic energy-wavelength diagram. Added to the figure are the typical size of objects to be studied and the energy of thermal neutrons.*

As the horizontal line at a wavelength of 1 Å shows, neutrons of this wavelength have an energy as low as about 80 meV, while 1 Å electrons correspond to about 150 eV and 1 Å photons (x-rays) have energies in excess of 12 keV. All three types of radiation

with this wavelength are well suited for scattering experiments on objects like atoms, molecules and crystals. The investigation (by scattering) of larger objects like colloids (in the 100 nm size range) requires, correspondingly, much lower energy probes like, for instance, photons in the ultraviolet range (about 12 eV).

The scattering process

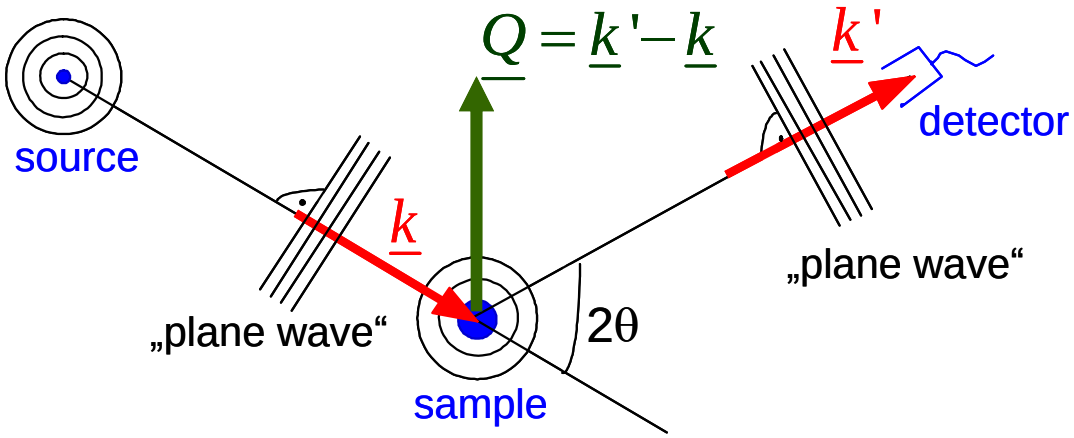

Fig. 4.3: *Sketch of the scattering process with the incoming wave characterized by wavevector $\underline{k}$, diffracted wave by $\underline{k}'$ and the sample by scattering vector $\underline{Q}$, assumed: plane waves, (Fraunhofer approximation, source-sample and sample-detector distances much larger than sample size), also assumed: monochromatic radiation (single wavelength)*

In the case of elastic scattering (diffraction) we have

$$k = |\underline{k}| = |\underline{k}'| = k' = \frac{2\pi}{\lambda} \qquad (4.1)$$

k is also called the wave number of the neutron and is conserved during scattering because the neutron energy and therefore the wavelength does not change.

The so-called *scattering vector* is defined by

$$\underline{Q} = \underline{k}' - \underline{k} \qquad (4.2)$$

The units of k, k' and Q are Å^{-1}.

$\hbar\underline{Q}$ represents the momentum transfer during scattering, since according to de Broglie, the momentum of the particle corresponding to the wave with wave vector $\underline{k}$ is given by $\underline{p}=\hbar\underline{k}$. The magnitude of the scattering vector can be calculated from wavelength λ and scattering angle 2θ as follows

$$Q = |\underline{Q}| = \sqrt{k^2 + k'^2 - 2kk'\cos 2\theta} \Rightarrow Q = \frac{4\pi}{\lambda}\sin\theta \qquad (4.3)$$

A scattering experiment comprises the measurement of the intensity distribution as a function of the scattering vector $I(\underline{Q})$. The scattered intensity is proportional to the so-

called *cross section*, where the proportionality factors arise from the detailed geometry of the experiment. For a definition of the scattering cross section see Figure 4.4.

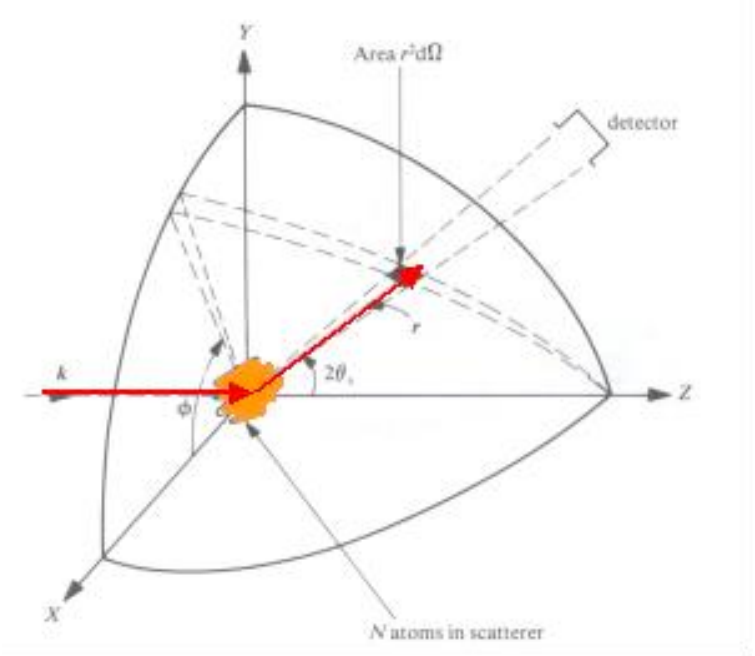

Fig. 4.4: *Geometry used for the definition of the scattering cross section.*

This is in close analogy to the absorption cross section derived in chapter 2.

Let us drop, for a moment, the assumption of strictly elastic scattering and treat the universal case of a general scattering experiment (will be needed in other chapters):
If n' particles are scattered per second into the solid angle $d\Omega$ seen by the detector under the scattering angle 2θ and into the energy interval between E' and $E' + dE'$, then we can define the so-called *double differential cross section* by:

$$\frac{d^2\sigma}{d\Omega dE'} = \frac{n'}{j d\Omega dE'} \tag{4.4}$$

Here j refers to the incident beam flux in terms of particles per area and time. If we are not interested in the change of the energy of the radiation during the scattering process, or if our detector is not able to resolve this energy change, then we will describe the angular dependence by the so-called *differential cross section:*

$$\frac{d\sigma}{d\Omega} = \int_0^\infty \frac{d^2\sigma}{d\Omega dE'} dE' \tag{4.5}$$

Finally the so-called *total scattering cross section* gives us a measure for the total scattering probability independent of changes in energy and scattering angle:

$$\sigma = \int_0^{4\pi} \frac{d\sigma}{d\Omega} d\Omega \tag{4.6}$$

All the information about the scattering matter is contained in the (double differential) scattering cross section. This includes positions and possible motions of scatterers in the sample volume. Note that in most diffraction experiments (with x-rays in particular, but also with electrons and neutrons), the actual measurement is energy-integrated because the detectors used are energy-insensitive. Consequently, the inelastic scattering also contributes to the measured intensity, but it is usually much weaker than the purely elastic scattering. Neutron scattering, however, offers the unique opportunity to set a very narrow energy window and study purely elastic scattering as well as inelastic scattering at arbitrary energies.
If we go back to elastic scattering the information on the positions of the scatterers is contained in the differential cross section $d\sigma / d\Omega$. The relationship between scattered intensity and the structure of the sample is particularly simple in the so-called *Born approximation*, which is often also referred to as *kinematic scattering approximation*. In this case, refraction of the beam entering and leaving the sample, multiple scattering events and the extinction of the primary beam due to scattering within the sample are being neglected. According to Figure 4.5, the phase difference between a wave scattered at the origin of the coordinate system and at position $\underline{r}$ is given by

$$\Delta\Phi = 2\pi \cdot \frac{\left(\overline{AB} - \overline{CD}\right)}{\lambda} = \underline{k}' \cdot \underline{r} - \underline{k} \cdot \underline{r} = \underline{Q} \cdot \underline{r} \qquad (4.7)$$

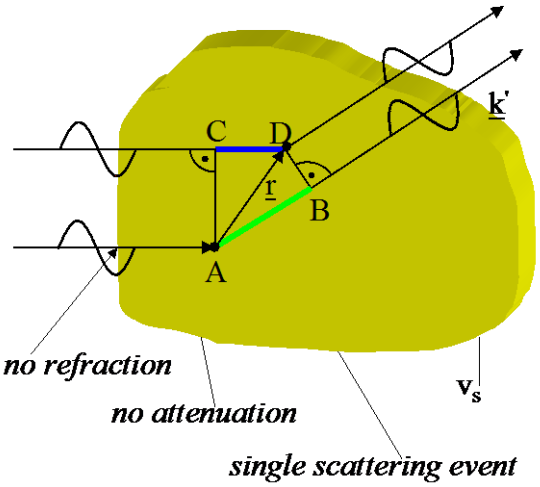

Fig. 4.5: *Elastic scattering from a non-periodic object, illustrating the phase difference between a beam scattered at the origin of the coordinate system (A) and a beam scattered at the position r. Additional caption: underlying assumptions of the kinematic scattering approximation.*

The scattered amplitude at position $\underline{r}$ is proportional to the scattering density $\rho_s(\underline{r})$ at this position. ρ_s depends on the type of radiation used and the interaction of this radiation with the sample. In fact, ρ_s is directly proportional to the interaction potential, as will be shown in the next paragraph. Assuming a laterally coherent beam, the total scattering amplitude is given by a coherent superposition of the scattering from all points within the sample, i. e. by the integral

$$A = A_0 \cdot \int_{V_S} \rho_S(\underline{r}) \cdot e^{i\underline{Q}\cdot\underline{r}} d^3r \qquad (4.8)$$

Here A_0 denotes the amplitude of the incident wave field. (4.8) demonstrates that the scattered amplitude is connected with the scattering density $\rho_s(\underline{r})$ by a simple Fourier transform. Knowledge of the scattering amplitude for all scattering vectors $\underline{Q}$ allows us to determine via a Fourier transform the scattering density uniquely. This is the complete information on the sample, which can be obtained by the scattering experiment. Unfortunately, nature is not so simple. On one hand, there is the technical problem that one is unable to determine the scattering cross section for all values of momentum transfer $\hbar\underline{Q}$. The more fundamental problem, however, is that normally the amplitude of the scattered wave is not measurable. Instead only the scattered intensity

$$I \sim |A|^2 \tag{4.9}$$

can be determined. Therefore the phase information is lost and the simple reconstruction of the scattering density via a reverse Fourier transform is no longer possible. This is the so-called *phase problem* of scattering. There are ways to overcome the phase problem, either experimentally, e. g. by use of reference waves (holography) or by using *a priori* information about the scattering density function (like positiveness or peakedness) which is the basis of the so called *direct methods of structure determination* that is very frequently used in x-ray crystallography. The question, which information we can obtain from a conventional scattering experiment despite the phase problem will be addressed below.

Which wavelength do we have to choose to obtain the required real space resolution? For information on a length scale L, a phase difference of about $Q \cdot L \approx 2\pi$ has to be achieved. Otherwise $\underline{k}'$ and $\underline{k}$ will not differ significantly (see eqn. (4.7)). According to (4.3) $Q \approx 2\pi/\lambda$ for typical scattering angles $(2\theta \sim 60°)$. Combining these two estimates, we end up with the requirement that the wavelength λ has to be on the order of the real space length scale L under investigation. To give an example: with the wavelength in the order of 0.1 nm, atomic resolution can be achieved in a scattering experiment.

Coherence

In the above derivation, we assumed plane waves as initial and final states. For a real scattering experiment, this is an unphysical assumption. In the incident beam, a wave packet is produced by collimation (defining the direction of the beam) and monochromatization (defining the wavelength of the incident beam). Neither the direction $\hat{\underline{k}}$, nor the wavelength λ have discrete values but rather have a distribution of non-vanishing width about their respective mean values. This wave packet can be described as a superposition of plane waves. As a consequence, the diffraction pattern will be a superposition of patterns for different incident wavevectors $\underline{k}$ and the question arises, which information is lost due to these non-ideal conditions. This *instrumental resolution* is intimately connected with the *coherence* of the beam. Coherence is needed, so that the interference pattern is not significantly destroyed. Coherence requires a phase relationship between the different components of the beam. Two types of coherence can be distinguished:

Temporal or longitudinal coherence due to a wavelength spread:

A measure for the longitudinal coherence is given by the length, on which two components of the beam with largest wavelength difference (λ and $\lambda+\Delta\lambda$) become fully out of phase.

According to the following figure, this is the case for $l_{\parallel} = n \cdot \lambda = \left(n - \frac{1}{2} \right)(\lambda + \Delta\lambda)$.

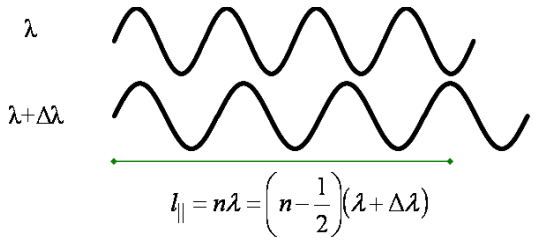

Fig. 4.6: *Sketch illustrating the longitudinal coherence due to a wavelength spread.*

From this, we obtain the *longitudinal coherence length* $l_{\parallel}$ as

$$l_{\parallel} = \frac{\lambda^2}{2\Delta\lambda} \qquad (4.10)$$

Transverse coherence due to source extension:
Due to the extension of the source (transverse beam size), the phase relation is destroyed for large source size or large divergence. According to the following figure, a first minimum occurs for $\frac{\lambda}{2} = d \cdot \sin\theta \approx d \cdot \theta$.

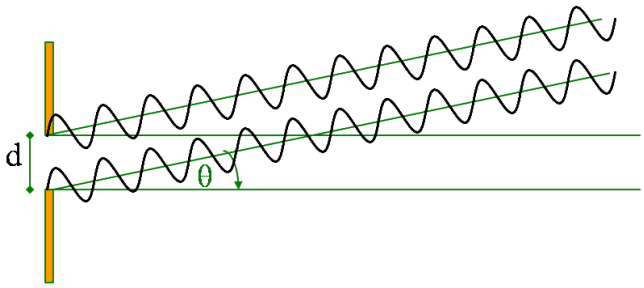

Fig. 4.7: *Sketch illustrating the transverse coherence due to source extension and beam divergence.*

From this, we obtain the *transversal coherence length* $l_{\perp}$ as

$$l_{\perp} = \frac{\lambda}{2\Delta\theta} \qquad (4.11)$$

Here $\Delta\theta$ is the divergence of the beam. Note that $l_{\perp}$ can be different along different spatial directions: in many instruments, the vertical and horizontal collimations are different.
Together, the longitudinal and the two transversal coherence lengths (in two directions perpendicular to the beam propagation) define a *coherence volume*. This is a measure for a volume within the sample, in which the amplitudes of all scattered waves superimpose to produce an interference pattern. Normally, the coherence volume is

significantly smaller than the sample size, typically a few *100 Å* for neutron scattering, up to *μm* for synchrotron radiation. Scattering between different coherence volumes within the sample is no longer coherent, i. e. instead of the amplitudes the intensities of the contributions to the scattering pattern have to be summed up. This limits the real space resolution of a scattering experiment to the extension of the coherence volume.

Neutron scattering from atomic nuclei

Neutrons interact with the nuclei of the atoms by potential scattering as well as with the magnetic moment of unpaired electrons in the electron shells of the atoms. Here we focus on the so-called nuclear scattering contribution. As the wavelength of thermal neutrons (approx. 10^{-10} m) is much larger than the diameter of the atomic nucleus (10^{-14} ...10^{-15} m), the atom is essentially a point scatterer. As the construction of Fig. 4.5 and equation (4.7) shows, this means that the length of the vector r (now a vector within the nucleus) is very small compared to the wavelength of the neutron and therefore the phase difference of waves from different parts of the nucleus is essentially zero. This is in sharp contrast to x-ray diffraction, where the scattering occurs from the electron cloud and the size of the scatterer and the wavelength of the radiation are similar. This results in the well-known formfactor falloff of the scattered intensity with increasing scattering angle. The same holds true for the magnetic formfactor for thermal neutrons. Magnetic neutron scattering will be the subject of chapter 7. For neutron scattering from the atomic nuclei, the formfactor is a constant. This is one big advantage of neutrons over x-rays because there is still an appreciable amount of scattered intensity even at very high scattering angles, where an x-ray experiment will yield hardly any useful information.

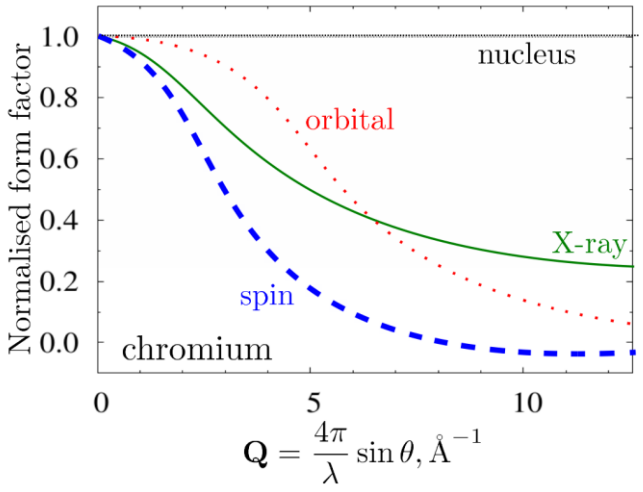

Fig. 4.8: *Form-factor of Cr [1]. On the Å length scale of the thermal neutron wavelength, the nucleus is point-like, therefore, nuclear scattering is independent of the scattering angle. For x-rays and magnetic neutron scattering, the form factor falls off with increasing scattering angle. For more details on magnetic neutron scattering see chapter 7.*

The interaction that governs nuclear neutron scattering (essentially potential scattering) is the strong nuclear force. Note that, despite the fact that the strong interaction of high

energy physics is responsible for the scattering of the neutron with the nucleus, the scattering probability is very small due to the small nuclear radius.
The quantity that describes the interaction between neutrons and matter is the scattering length b, it is usually expressed in units of a Fermi (1 fm = 10^{-15} m). Another frequently used quantity is the total cross section of a given nucleus $\sigma = 4\pi|b|^2$ corresponding to the surface area of a sphere with radius *b*. σ is usually expressed in barns, 1 barn = 10^{-24} cm^2. A simple description of potential scattering predicts the smooth increase of the scattering length with increasing atomic weight depicted in Figure 4.9 by the dashed line. Obviously, this description is rather crude as resonance effects play an important role and, consequently, there are pronounced deviations from this line. As the interaction potential depends on the details of the nuclear structure, scattering lengths *b* can be very much different for different isotopes of the same element and also for different nuclear spin states (see chapter 7). In fact, neutron nuclear scattering lengths are still very hard to calculate (in contrast to x-ray scattering where the scattering power of any atom can be calculated to a very high precision) illustrating our still quite limited knowledge of the nuclear structure of atoms as opposed to the very well understood electronic structure of atoms. Consequently, the tabulated values of *b* which can be found in [2] or at http://www.ncnr.nist.gov/resources/n-lengths/ are experimentally measured quantities, not calculated ones. The scattering length is mostly positive but can also adopt negative values, this negative sign corresponds to a phase shift of π (or 180°) during the scattering process. The fact that different isotopes of the same element have different scatterings lengths also gives rise to the appearance of so-called *incoherent scattering* (see below).

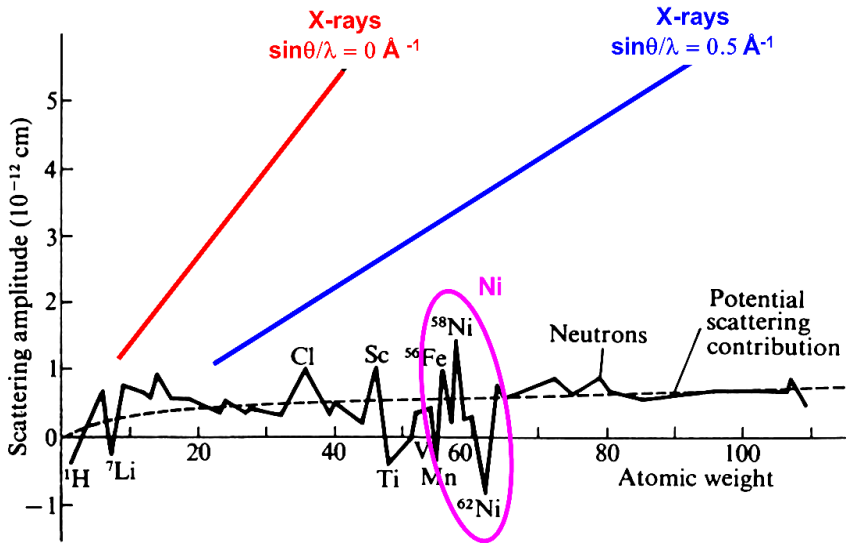

Fig. 4.9: *Scattering length as a function of atomic weight throughout the periodic table (from Research, London 7 (1954), 257). Note the two different curves for x-rays at low- and high scattering angles, illustrating the formfactor falloff that is typical for x-rays but doesn't exist for nuclear neutron scattering.*

In Figure 4.10, the scattering cross sections for x-rays and neutrons are compared. Note that the x-ray scattering cross sections are in general a factor of 10 larger as compared to the neutron scattering cross sections. This means that the signal for x-ray scattering is stronger for the same incident flux and sample size. For x-rays, the

cross section depends on the number of electrons and thus varies in a monotonic fashion throughout the periodic table. Clearly it will be difficult to determine hydrogen positions with x-rays in the presence of heavy elements such as metal ions. Moreover, there is a very weak contrast between neighboring elements as can be seen for the transition metals Mn, Fe and Ni in Figure 4.10. However, this contrast can be enhanced by anomalous scattering, if the photon energy is tuned close to the absorption edge of an element. For neutrons the cross section depends on the details of the nuclear structure and thus varies in a non-systematic fashion throughout the periodic table. As an example, there is a very high contrast between Mn and Fe. With neutrons, the hydrogen atom is clearly visible even in the presence of such heavy elements as Uranium. Moreover there is a strong contrast between the two Hydrogen isotopes H and D. This fact can be exploited for soft condensed matter investigations by selective deuteration of certain molecules or functional groups. This will vary the contrast within the sample.

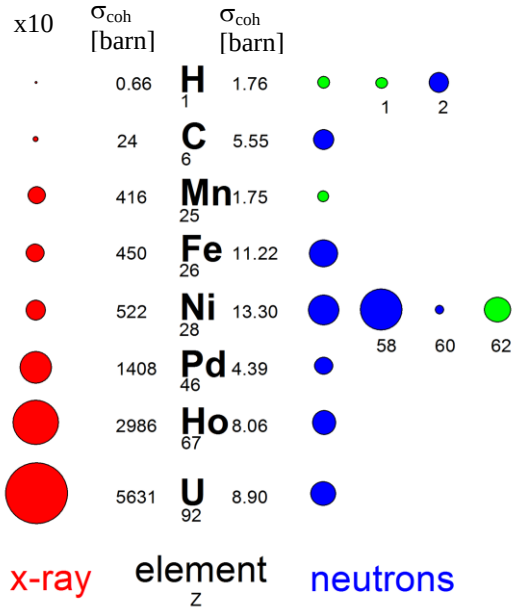

Fig. 4.10: *Comparison of the (coherent) scattering cross-sections σ for x-rays and neutrons for a selection of elements. The area of the colored circles represent the scattering cross section, where in the case of x-rays a scale factor 10 has to be applied. For neutrons, the blue and green circles distinguish the cases where the scattering occurs with or without a phase shift of π. For $_1$H and $_{28}$Ni, scattering cross sections for certain isotopes are given in addition to the averaged values for the natural abundances.*

Coherent and incoherent scattering

As mentioned above, the scattering length *b* is different for different isotopes of a given element and also for different nuclear spin states. This gives rise to an additional contribution to the total intensity, the *incoherent scattering*. In this chapter, we will

focus on *isotope-incoherence* and leave the detailed discussion of *spin-incoherence* for other chapters.

Figure 4.11 shows a 2-D model crystal with atoms of two isotopes of the same element with two different scattering lengths b_i sitting on fixed positions $\underline{R}_i$ in a crystal lattice. As stated above, the scattering amplitude is obtained from a Fourier transform:

$$A(\underline{Q}) = \sum_i b_i e^{i\underline{Q}\cdot\underline{R}_i} \tag{4.12}$$

When we calculate the scattering cross section, we have to take into account that the different isotopes are distributed randomly over all sites. Therefore, we have to average over the random distribution of the scattering length in the sample:

$$\frac{d\sigma}{d\Omega}(\underline{Q}) \sim \left|A(\underline{Q})\right|^2 = \left\langle \sum_i b_i \; e^{i\underline{Q}\cdot\underline{R}_i} \cdot \sum_j b_j^* e^{-i\underline{Q}\underline{R}_j} \right\rangle \tag{4.13}$$

As isotopes of the same element are chemically undistinguishable, the distribution of the scattering lengths b_i and b_j on the different sites is completely uncorrelated. This implies that for $i \neq j$, the expectation value of the product equals to the product of the expectation values. Only for $i = j$ a correlation occurs, which gives an additional term describing the mean quadratic deviation from the average:

$$\left\langle b_i b_j \right\rangle = \begin{cases} \langle b\rangle\langle b\rangle = \langle b\rangle^2 & i \neq j \\ \left\langle b^2 \right\rangle = \langle b\rangle^2 + \left\langle \left(b - \langle b\rangle\right)^2 \right\rangle & i = j \end{cases} \tag{4.14}$$

The line for i = j results from the identity:

$$\left\langle \left(b - \langle b\rangle\right)^2 \right\rangle = \left\langle b^2 - 2b\langle b\rangle + \langle b\rangle^2 \right\rangle = \left\langle b^2 \right\rangle - \langle b\rangle^2 \tag{4.15}$$

Therefore, we can write the cross section in the following form:

$$\begin{aligned} \frac{d\sigma}{d\Omega}(\underline{Q}) &= \langle b\rangle^2 \left| \sum_i e^{i\underline{Q}\cdot\underline{R}_i} \right|^2 \qquad \text{"}coherent\text{"} \\ &+ N\left\langle \left(b - \langle b\rangle\right)^2 \right\rangle \qquad \text{"}incoherent\text{"} \end{aligned} \tag{4.16}$$

The scattering cross section is a sum of two terms. Only the first term contains the phase factors $e^{i\underline{Q}\cdot\underline{R}}$, which result from the coherent superposition of the scattering from pairs of scatterers. This term takes into account interference effects and is therefore named *coherent scattering*. The scattering length averaged over the isotope- and nuclear spin-distribution enters this term. This is in complete analogy to the "isotope insensitive" x-ray-diffraction. The second term in (4.16) does not contain any phase information and is proportional to the number N of atoms (and not to N^2). This term is not due to the interference of scattering from different atoms and it has no direct counterpart in x-ray scattering. As we can see from (4.14) (line $i = j$), this term corresponds to the scattering from single atoms, which subsequently superimpose in an incoherent manner (adding intensities, not amplitudes!). This is the reason for the intensity being proportional to the number N of atoms. Therefore the second term is called *incoherent scattering*.

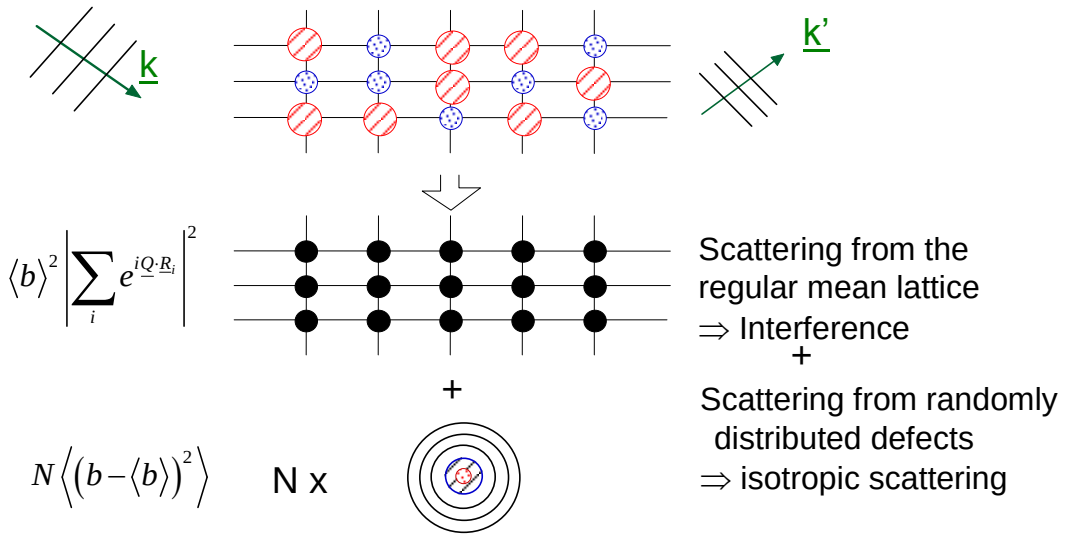

Fig. 4.11: *Upper panel: Sketch of the scattering process from a 2-D lattice of N chemically identical atoms with two isotopes (small dotted circles and large hatched circles). The area of the circle represents the scattering cross section of the single isotope. Middle panel: The incident wave is scattered coherently only from the average structure. This gives rise to Bragg peaks in certain directions. Lower panel: Additionally, an isotropic background (incoherent scattering) is observed, which is proportional to the number N of atoms and to the mean quadratic deviation from the average scattering length.*

The most prominent example for *isotope incoherence* is elementary nickel. The scattering lengths of the nickel isotopes are listed together with their natural abundance in Table 4.1 [2]. The differences in the scattering lengths for the various nickel isotopes are enormous. Some isotopes even have negative scattering lengths. This is due to resonant bound states, as compared to the usual potential scattering.

Isotope	Natural Abundance	Nuclear Spin	Scattering Length [fm]
^{58}Ni	68.27 %	0	14.4(1)
^{60}Ni	26.10 %	0	2.8(1)
^{61}Ni	1.13 %	$^{3}/_{2}$	7.60(6)
^{62}Ni	3.59 %	0	-8.7(2)
^{64}Ni	0.91 %	0	-0.37(7)
Ni			10.3(1)

Tab. 4.1: *The scattering lengths of the nickel isotopes and the resulting scattering length of natural $_{28}$Ni [2], see also fig. 4.9.*

Neglecting the less abundant isotopes ^{61}Ni and ^{64}Ni, the average scattering length is calculated as:

$$\langle b \rangle \approx \left[0.68 \cdot 14.4 + 0.26 \cdot 2.8 + 0.04 \cdot (-8.7)\right] fm \approx 10.2\, fm \qquad (4.17)$$

which gives the total coherent cross section of:

$$\Rightarrow \sigma_{coherent} = 4\pi\langle b\rangle^2 \approx 13.1\,barn\ (exact: 13.3(3) barn) \tag{4.18}$$

The incoherent scattering cross section per nickel atoms is calculated from the mean quadratic deviation:

$$\sigma_{incoherent}^{Isotope} = 4\pi\left[0.68\cdot(14.4-10.2)^2 + 0.26\cdot(2.8-10.2)^2 + 0.04\cdot(-8.7-10.2)^2\right] fm^2 \tag{4.19}$$
$$\approx 5.1 barn\ (exact: 5.2(4) barn)$$

Values in parentheses are the exact values taking into account the isotopes ^{61}Ni and ^{64}Ni and the nuclear spin incoherent scattering (see chapter 7). From (4.18) and (4.19), we learn that the incoherent scattering cross section in nickel amounts to more than one third of the coherent scattering cross section.

The most prominent example for *nuclear spin incoherent scattering* is elementary hydrogen. The nucleus of the hydrogen atom, the proton, has the nuclear spin $I = ½$. The total nuclear spin of the system H + n can therefore adopt two values: $J = 0$ and $J = 1$. Each state has its own scattering length: b_- for the singlet state $(J = 0)$ and b_+ for the triplet state $(J = 1)$.

Total Spin	Scattering Length	Abundance
J = 0	b_- = - 47.5 fm	$\frac{1}{4}$
J = 1	b_+ = 10.85 fm	$\frac{3}{4}$
<b> = - 3.739(1) fm		

Tab. 4.2: *Scattering lengths for hydrogen [2].*

As in the case of isotope incoherence, the average scattering length can be calculated:

$$\langle b\rangle = \left[\frac{1}{4}(-47.5) + \frac{3}{4}\cdot(10.85)\right] fm = -3.74\, fm \tag{4.20}$$

This corresponds to a coherent scattering cross section of about ≈ 1.76 barn [2]:

$$\Rightarrow \sigma_{coherent} = 4\pi\langle b\rangle^2 = 1.7568(10)\, barn \tag{4.21}$$

The nuclear spin incoherent part is again given by the mean quadratic deviation from the average:

$$\sigma_{incoherent}^{nuclear\ spin} = 4\pi\left[\frac{1}{4}(-47.5+3.74)^2 + \frac{3}{4}(10.85+3.74)^2\right] fm^2 = 80.2\, barn$$

(*exact value:* 80.26(6) *barn*) (4.22)

Comparing (4.21) and (4.22), it is immediately clear that hydrogen scatters mainly incoherently. As a result, we observe a large background for all samples containing hydrogen. We should avoid all hydrogen containing glue for fixing our samples to a sample stick. Finally, we note that deuterium with nuclear spin $I = 1$ has a much more favorable ratio between coherent and incoherent scattering:

$$\sigma_{coh.}^{D} = 5.592(7) barn; \quad \sigma_{inc.}^{D} = 2.05(3) barn$$

The coherent scattering lengths of hydrogen (-3.74 fm) and deuterium (6.67 fm) are significantly different. This can be used for contrast variation by isotope substitution in all samples containing hydrogen, i. e. in biological samples or soft condensed matter samples, see the corresponding chapters.

A further important element, which shows strong nuclear incoherent scattering, is vanadium. Natural vanadium consists to 99,75 % of the isotope ^{51}V with nuclear spin 7/2. By chance, the ratio between the scattering lengths b_+ and b_- of this isotope are approximately equal to the reciprocal ratio of the abundances. Therefore, the coherent scattering cross section is very small and the incoherent cross section dominates [2]:

$$\sigma_{coh}^{V} = 0.01838(12)\,barn; \quad \sigma_{incoh}^{V} = 5.08(6)\,barn$$

For this reason, Bragg scattering of vanadium is difficult to observe above the large incoherent background. On the other hand, this fact can be turned into an advantage: By using vanadium metal, one can make sample containers which are practically invisible for (coherent) neutron scattering: They produce almost no reflections but rather a diffuse background (since incoherent scattering is isotropic) which usually doesn't cause severe problems in diffraction experiments.

4.3 Diffraction geometry

For purely elastic scattering, the scattering function $S(\underline{Q},\omega)$ reduces to the special case without energy transfer ($E_0 = E_1$ and $\hbar\varpi = E_0 - E_1 = 0$) and equal length of the wave vectors of the incident and scattered beams ($|\underline{k}_0| = |\underline{k}_1|$). $S(\underline{Q},\omega = 0)$ and the scattering intensity then only depends on the scattering vector $\underline{Q} = \underline{k}_0 - \underline{k}_1$. The *coherent elastic* neutron scattering (≡ neutron *diffraction*) yields information on the positions (distribution) of the atomic nuclei and the arrangement of the localised magnetic spins in crystalline solids, the pair correlation function of liquids and glasses, and the conformation of polymer chains.

Figure 4.12 shows a sketch of a general diffraction experiment. More specifically, it is a typical setup of a constant wavelength, angular dispersive diffraction experiment. There are other methods to perform a diffraction experiment (e.g. time of flight- (TOF-), Laue-, energy-dispersive diffractometers etc.) but these are outside the scope of this introductory lecture.

For constant wavelength diffraction, the energy (wavelength) and direction (collimation) of the incident neutron beam needs to be adjusted. For that purpose, the diffractometer is equipped with a crystal monochromator to select a particular wavelength band ($\lambda \pm \Delta\lambda/\lambda$) out of the "white" beam. Collimators are used to define the beam direction and divergence pretty much as is done in x-ray diffraction.

In the case of a crystalline sample, the diffraction geometry is most conveniently described by the concepts of the *reciprocal lattice* and the *Ewald construction* which are both well-known from x-ray-diffraction.

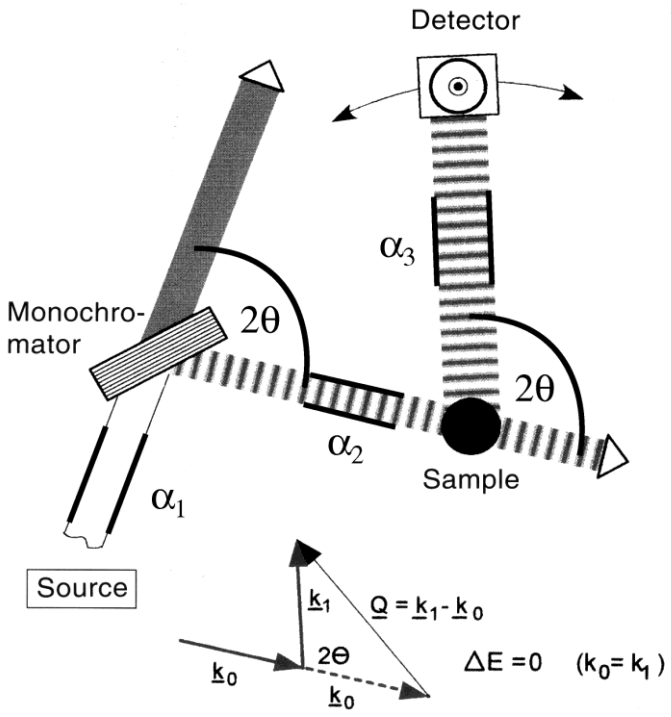

Fig. 4.12: *Schematic representation of a constant wavelength diffractometer.*

Reciprocal lattice

The characteristic feature of the crystalline state (see chapter 3) is its periodic order, which may be represented by a (translation) lattice. In the 3D case, three basis vectors $\boldsymbol{a_1}$, $\boldsymbol{a_2}$, $\boldsymbol{a_3}$ define a parallelepiped, called unit cell. Each lattice node of the crystal lattice can be addressed by a general lattice vector

$$\boldsymbol{a} = u\,\boldsymbol{a_1} + v\,\boldsymbol{a_2} + w\,\boldsymbol{a_3}. \tag{4.23}$$

which results from a linear combination of the basis vectors with coefficients *u*, *v*, and *w* (positive or negative integers, including 0).

The position of atom j in the unit cell is given by the vector

$$\boldsymbol{r_j} = x_j\,\boldsymbol{a_1} + y_j\,\boldsymbol{a_2} + z_j\,\boldsymbol{a_3}. \tag{4.24}$$

The coefficients x_j, y_j, and z_j are called atomic coordinates ($0 \le x_j < 1$; $0 \le y_j < 1$; $0 \le z_j < 1$).

For an ideal crystal and an infinite lattice with the basis vectors $\boldsymbol{a_1}$, $\boldsymbol{a_2}$, $\boldsymbol{a_3}$ there is only diffraction intensity $I(\boldsymbol{\tau})$ at the vectors

$$\boldsymbol{\tau} = h\,\boldsymbol{\tau_1} + k\,\boldsymbol{\tau_2} + l\,\boldsymbol{\tau_3}. \tag{4.25}$$

of the reciprocal lattice. *h,k,l* are the integer Miller indices and $\boldsymbol{\tau_1}$, $\boldsymbol{\tau_2}$, $\boldsymbol{\tau_3}$ are the basis vectors of the reciprocal lattice, satisfying the two conditions

$$\boldsymbol{\tau_1}\cdot\mathbf{a_1} = \boldsymbol{\tau_2}\cdot\mathbf{a_2} = \boldsymbol{\tau_3}\cdot\mathbf{a_3} = 1 \text{ and } \boldsymbol{\tau_1}\cdot\mathbf{a_2} = \boldsymbol{\tau_1}\cdot\mathbf{a_3} = \boldsymbol{\tau_2}\cdot\mathbf{a_1} = \ldots = 0,$$

or in terms of the Kronecker symbol with i, j and k = 1, 2, 3

$$\delta_{ij} = 0 \text{ for } i \neq j \text{ and } \delta_{ij} = 1 \text{ for } i = j \text{ with } \delta_{ij} = \boldsymbol{\tau_i}\cdot\boldsymbol{\tau_j}. \tag{4.26}$$

The basis vectors of the reciprocal lattice can be calculated from those of the unit cell in real space

$$\boldsymbol{\tau}_i = (\mathbf{a_j} \times \mathbf{a_k})/V_c, \tag{4.27}$$

where × means the cross product, and $V_c = \mathbf{a_1}\cdot(\mathbf{a_2}\times\mathbf{a_3})$ is the volume of the unit cell.

In solid state physics,

$$\boldsymbol{Q} = 2\pi\ \boldsymbol{\tau} \tag{4.28}$$

is used instead of $\boldsymbol{\tau}$

Here is a compilation of some properties of the reciprocal lattice:

- Each reciprocal lattice vector is perpendicular to two real space vectors: $\boldsymbol{\tau}_i \perp \mathbf{a_j}$ and $\mathbf{a_k}$ (for $i \neq j, k$)
- The lengths of the reciprocal lattice vectors are $|\boldsymbol{\tau}_i| = 1/V_c \cdot |\mathbf{a_j}| \cdot |\mathbf{a_k}| \cdot \sin\angle(\mathbf{a_j},\mathbf{a_k})$.
- Each point *hkl* in the reciprocal lattice refers to a set of planes (*hkl*) in real space.
- The direction of the reciprocal lattice vector $\boldsymbol{\tau}$ is normal to the (*hkl*) planes and its length is reciprocal to the interplanar spacing d_{hkl}: $|\boldsymbol{\tau}| = 1/d_{hkl}$.
- Duality principle: The reciprocal lattice of the reciprocal lattice is the direct lattice.

Performing a diffraction experiment on a single crystal actually means doing a Fourier transform of the 3D-periodic crystal (see chapter on symmetry in crystals) followed by forming the square of the resulting (complex) amplitude function. The Fourier transform of the (infinite) crystal lattice is essentially the reciprocal lattice derived above and yields directly the positions of the reflections in space (directions of the diffracted beams). The atomic arrangement within the unit cell determines the reflection intensities which may be envisaged as a weight attached to the nodes of the reciprocal lattice.

Doing a (single crystal) diffraction experiment therefore corresponds to measuring the positions and weights of the reciprocal lattice points. Their position yields information on the lattice parameters and the orientation of the crystal on the diffractometer while the weights (the reflection intensities) allow reconstructing the atomic positions within the unit cell.

Ewald construction

The concept of the reciprocal space also provides a handy tool to express geometrically the condition for Bragg scattering in the so-called Ewald construction. In this way the different diffraction methods can be discussed.

We consider the reciprocal lattice of a crystal and choose its origin 000. In Fig. 4.13 the wave vector $\underline{k}_0$ (defined in the crystallographers' convention with $|\underline{k}_0| = 1/\lambda$) of the incident beam is marked with its end at 000 and its origin P. We now draw a sphere of radius $|\underline{k}_0| = 1/\lambda$ around P passing through 000. Now, if any point *hkl* of the reciprocal lattice lies on the surface of this "Ewald sphere", then the diffraction condition for the (*hkl*) set of lattice planes is fulfilled: The wave vector of the diffracted beam $\underline{k}$ **(**with its origin also at P) for the set of planes (*hkl*), is of the same length as $\underline{k}_0$ ($|\underline{k}| = |\underline{k}_0|$) and the resulting vector diagram satisfies $\underline{k} = \underline{k}_0 + \boldsymbol{\tau}$. Introducing the scattering angle 2θ (and

hence the Bragg angle θ_{hkl}), we can deduce immediately from $2|\underline{k}|\cdot\sin\theta = |\boldsymbol{\tau}|$ the Bragg equation $2d_{hkl}\cdot\sin\theta_{hkl} = \lambda$.

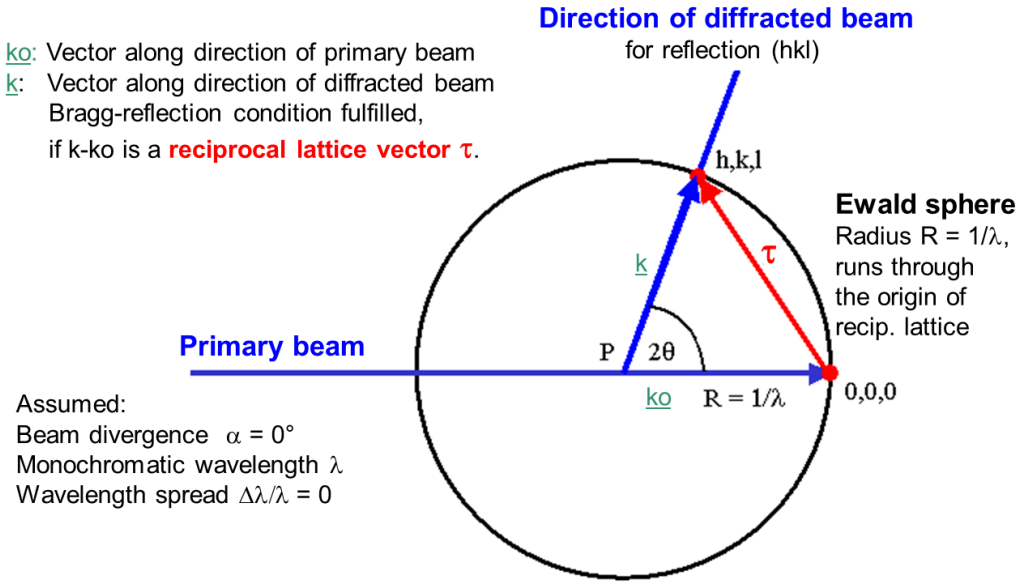

Fig. 4.13: *Ewald construction in reciprocal space, showing the diffraction condition for reflection (hkl).*

In the case of single crystal diffraction a rotation of the crystal and therefore also of the corresponding reciprocal lattice (which is rigidly attached to the crystal) is often used to set the diffraction conditions for the measurement of intensities $I(\boldsymbol{\tau})$.

If $|\boldsymbol{\tau}| > 2/\lambda$ (then $d_{hkl} < \lambda/2$) the reflection *hkl* cannot be observed. This condition defines the so called limiting sphere, with center at 000 and radius $2/\lambda$: only the points of the reciprocal lattice inside the limiting sphere can be rotated into diffraction positions. Vice versa if $\lambda > 2d_{max}$, where d_{max} is the largest interplanar spacing of the unit cell, then the diameter of the Ewald sphere is smaller than $|\boldsymbol{\tau}|_{min}$. Under these conditions no node of the reciprocal lattice can intercept the Ewald sphere. That is the reason why diffraction of visible light (wavelength ≅ 5000 Å) can never be obtained from crystals. λ_{min} determines the amount of information available from a diffraction experiment. In ideal conditions λ_{min} should be short enough to measure all points of the reciprocal lattice with significant diffraction intensities.

For a real crystal of limited perfection and size the infinitely sharp diffraction peaks (delta functions) evolve into broadened reflections. One reason can be the local variation of the orientation of the crystal lattice (mosaic spread) implying some angular splitting of the vector $\boldsymbol{\tau}$. A spread of interplanar spacings $\Delta d/d$, which may be caused by some inhomogeneities in the chemical composition of the sample, gives rise to a variation of its magnitude $|\boldsymbol{\tau}|$. The ideal diffraction geometry on the other hand also needs to be modified: In a real experiment the primary beam has a non-vanishing divergence and wavelength spread. The detector aperture is also finite. A gain of intensity, which can be accomplished by increasing the angular divergence and wavelengths bandwidth, has to be paid for by some worsening of the resolution function

(see below) and hence by a limitation of the ability to separate different Bragg reflections.

All of these influences can be studied by the Ewald construction. The influence of a horizontal beam divergence on the experimental conditions for a measurement of Bragg-intensities of a single crystal is illustrated in Fig. 4.14 where strictly monochromatic radiation (only one wavelength λ with $\Delta\lambda/\lambda = 0$) is assumed. To collect the complete intensity contained in the spread out reflection, a so-called ω-scan, where the crystal is rotated around the sample axis perpendicular to the diffraction plane, may be used. The summation over the whole reflection profile yields the so-called integral diffraction intensities.

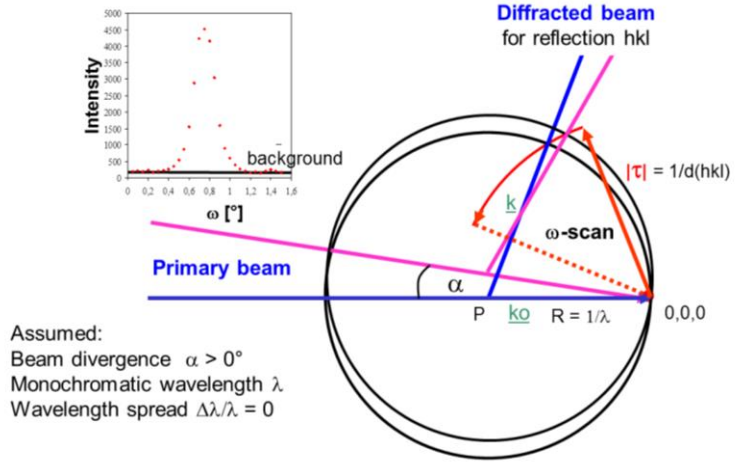

Fig. 4.14: *Ewald-construction: Influence of the horizontal beam divergence on the experimental conditions for the measurement of Bragg-intensities.*

Finally, the geometry of powder diffraction experiments can also be discussed in terms of the Ewald-construction:

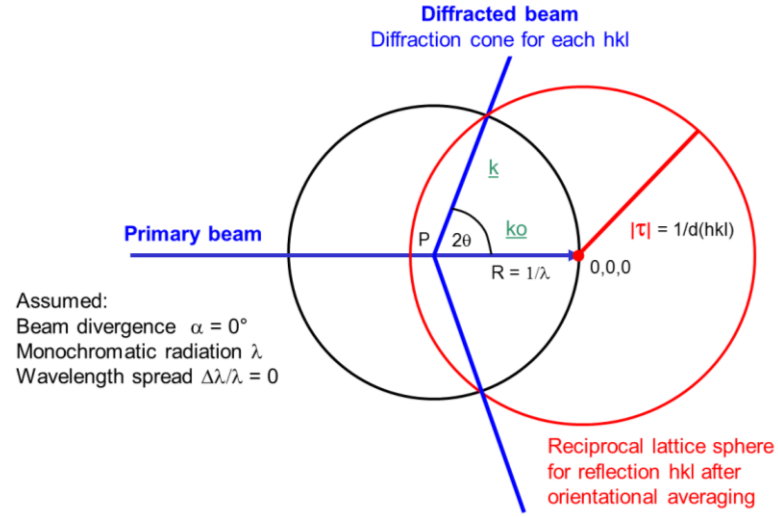

Fig. 4.15: *Ewald construction for a powder diffraction experiment.*

An ideal polycrystalline sample is characterised by a very large number of arbitrarily oriented small crystallites. Therefore, the reciprocal lattice point hkl is smeared out on a sphere and the 3D-information contained in vector $\boldsymbol{\tau}$ is reduced to only 1D-information contained in $|\boldsymbol{\tau}|$. In Figure 4.15 the corresponding sphere with radius $|\boldsymbol{\tau}| = 1/d_{hkl}$ is drawn around the origin of the reciprocal lattice at 0,0,0. For each Bragg-reflection the circle of intersection of the "reciprocal lattice sphere" with the Ewald-sphere yields a diffraction cone. These cones are recorded on a point or position sensitive detector. And the resulting information is plotted as a intensity vs. diffraction angle (or Q) diagram. All reflections with equal interplanar spacing d_{hkl} are perfectly superimposed and cannot be separated experimentally.

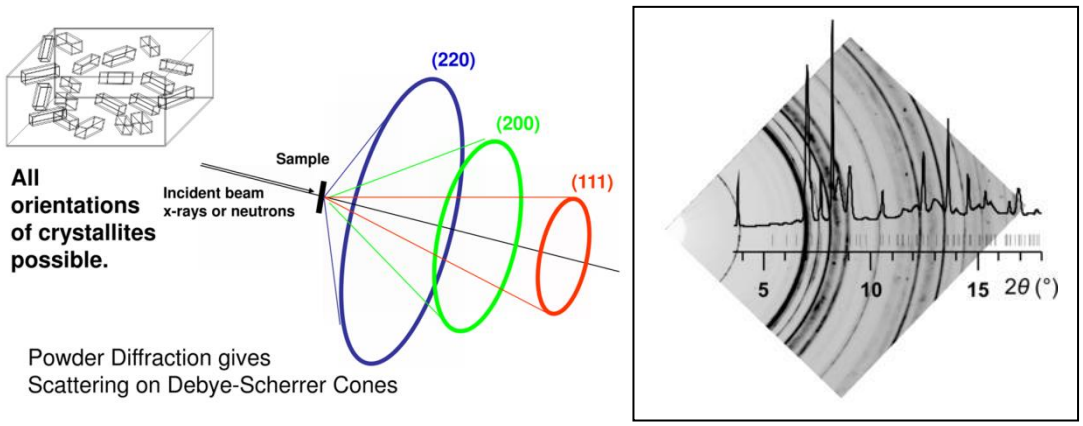

Fig. 4.16: *Sketch of a powder diffraction experiment, diffraction cones are recorded on a 2D- or 1D- detector (reproduced from [3]).*

4.4 Diffraction intensities

As stated in chapter 4.2, a scattering experiment is equivalent to performing a Fourier transform of the scattering object (eqn. 4.8) followed by taking the square of the resulting complex amplitude (eqn. 4.9). The latter step is very simply due to the fact, that our detectors can measure the magnitude (the absolute value) of a diffracted wave but are completely insensitive to its phase. This results in an intrinsic loss of information and poses the so-called "phase problem of crystallography". There are methods to reconstruct the missing phase information from the measured magnitudes and from a-priori information about the scattering object (e.g. the so-called direct methods of *structure determination*), but these methods are again outside the scope of this lecture. The first step of a diffraction experiment - the Fourier transform - needs some further elaboration: In a diffraction (elastic, coherent scattering) experiment we can safely ignore time as a variable and concentrate only on the spatial Fourier transform of the scattering object (here: the crystal). For those who are not particularly familiar with the Fourier transform, figure 4.17 shows a very simple one-dimensional analogue. The transformation from A to E (labelled FT, ||) corresponds to the diffraction experiment: Fourier-transform (harmonic analysis) plus calculation of the absolute value. If we could also retrieve the phases φ, the inverse Fourier transform (labelled FT^{-1}, φ) would lead directly to the structure of the scattering object A (harmonic synthesis).

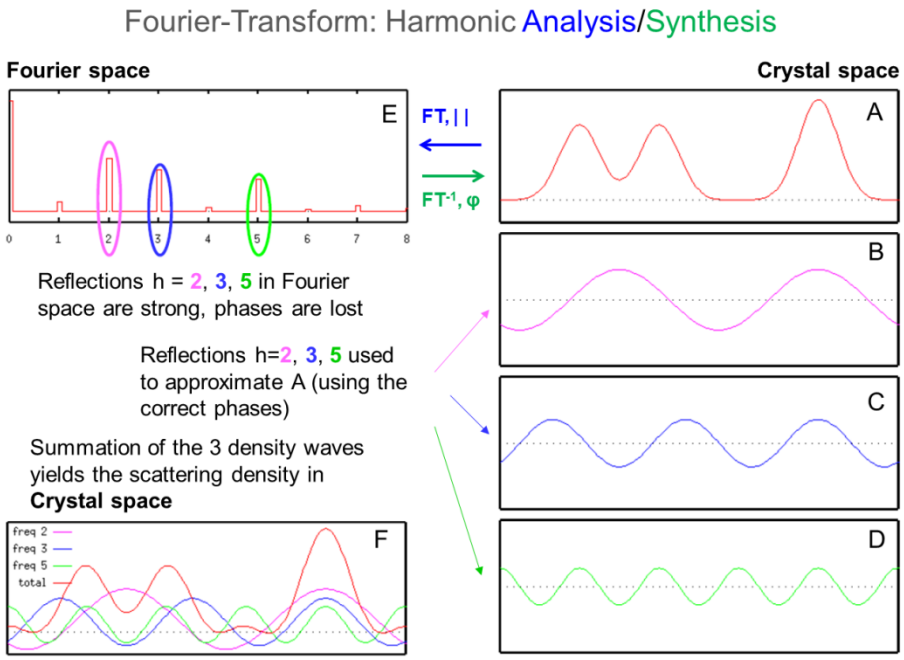

Fig. 4.17: *1D illustration of the Fourier transform, A: scattering object: 1D-density function, assumed: periodic in 1D, B-D: decomposition of A into 3 harmonic (co-)sine waves, F: synthesis of A (red curve) via summation of B-D with the correct phases, E: "diffractogramm" of A: Fourier transform, only the magnitudes of waves in B to D are plotted, figures taken from[4].*

Without the phase information, we need an approximate model of the crystal structure and a formula to calculate diffraction intensities from the model. In the kinematical approximation (see above) we use the so called structure factor formula for that purpose (see below). The model is then iteratively improved to give an optimum match between observed and calculated intensities. This is referred to as the *structure refinement*.

Structure factor and Bragg intensities

In the kinematical approximation, which assumes that the magnitude of the incident wave amplitude is the same at all points in the specimen (this implies a small sample size, weak scattering intensities, no multiple diffraction and negligible absorption), the diffracted intensity is proportional to the square of the amplitude of the scattered wave for each individual reflection; it can be regarded as a weight ascribed to the reciprocal-lattice nodes (see eqn. 4.25).

$$I(\boldsymbol{\tau}) \sim |\boldsymbol{F}(\boldsymbol{\tau})|^2. \qquad (4.29)$$

The structure factor $\mathbf{F}(\boldsymbol{\tau})$ is the Fourier transform of the scattering density within the unit cell. For a 3D-periodic scattering density function composed of discrete atoms (the crystal), the integral in (4.8) describing the Fourier transform in its most general form, simplifies to a sum over all atoms j in the unit cell The structure factor $\mathbf{F}(\boldsymbol{\tau})$ contains the complete structural information, including the atomic coordinates $\boldsymbol{r_j} = x_j\, \boldsymbol{a_1} + y_j\, \boldsymbol{a_2} + z_j\, \boldsymbol{a_3}$ (see eqn. 4.24), site occupations and the thermal vibrations contained in T_j.

$$\boldsymbol{F}(\boldsymbol{\tau}) = \sum_j bj \cdot \exp[2\pi i(\boldsymbol{\tau} \cdot \boldsymbol{r}_j)] \cdot T_j(\boldsymbol{\tau}) = |\boldsymbol{F}(\boldsymbol{\tau})| \cdot \exp[i\varphi(\boldsymbol{\tau})]. \quad (4.30)$$

In the case of nuclear scattering of neutrons the structure factor has the dimension of a length, as has the scattering length $b_j(\boldsymbol{\tau}) = b_j$ = const. of nucleus j. $T_j(\boldsymbol{\tau})$ is the Debye-Waller factor which takes into account dynamical and static displacements of the nucleus j from its average position $\boldsymbol{r}_j$ in the unit cell. With the fractional coordinates x_j, y_j and z_j, the scalar product in the exponential function can be written as

$$\boldsymbol{\tau} \cdot \boldsymbol{r}_j = hx_j + ky_j + lz_j \quad (4.31)$$

In a diffraction experiment normally only relative Bragg intensities are measured. A scale factor SCALE takes into account all parameters which are constant for a given set of diffraction intensities. Additional corrections have to be applied, which are a function of the scattering angle. For nuclear neutron diffraction from single crystals the integrated relative intensities are given by

$$I(\boldsymbol{\tau}) = \text{SCALE} \cdot L \cdot A \cdot E \cdot |\boldsymbol{F}(\boldsymbol{\tau})|^2 \quad (4.32)$$

The Lorentz factor L is instrument specific. The absorption correction A depends on the geometry and linear absorption coefficient of the sample and the extinction coefficient E takes into account a possible violation of the assumed conditions for the application of the kinematical diffraction theory.

Information on the crystal system, the Bravais lattice type and the basis vectors $\boldsymbol{a_1}$, $\boldsymbol{a_2}$, $\boldsymbol{a_3}$ of the unit cell (lattice parameters a, b, c, α, β, γ) may be directly deduced from the reciprocal lattice. The $|\boldsymbol{F}(\boldsymbol{\tau})|^2$ values associated as weights to the nodes of the reciprocal lattice give the diffraction symbol and hence valuable information on the space-group symmetry (see chapter 3). Here, systematic absences (zero structure factors) can be used to determine non-primitive Bravais lattices or detect the presence of non-symmorphic symmetry operations (symmetry operations with translation components).

As an example, consider a *body centered cubic* lattice with atoms at 0,0,0 and ½,½,½. Using eqn. 4.31 and dropping the Debye-Waller factor for the moment, eqn. 4.30 may be rewritten as:

$$\boldsymbol{F}(hkl) = \sum_j bj \cdot \exp[2\pi i(hx_j + ky_j + lz_j)] \cdot T_j(\boldsymbol{\tau}) = |\boldsymbol{F}(\boldsymbol{\tau})| \cdot \exp[i\varphi(\boldsymbol{\tau})]. \quad (4.33)$$

For a centrosymmetric structure, F is a real quantity (instead of complex), the exponentials in (4.33) reduce to cosines and the phase factor assumes only the values + or -. For this simple structure, index j just runs over the two equivalent atoms with scattering length b within the unit cell. Thus we get:

$$F(hkl) = b \cdot \cos\left[2\pi(h \cdot 0 + k \cdot 0 + l \cdot 0\right] + b \cdot \cos\left[2\pi(h/2 + k/2 + l/2)\right] \quad (4.34)$$

The first term cos(0) = 1 and we therefore have:

$$F(hkl) = b + b \cdot \cos\left[2\pi(h/2 + k/2 + l/2)\right] = b \cdot (1 + \cos[\pi(h + k + l)]) \quad (4.35)$$

If h+k+l is even, the cosine term is +1, otherwise it is -1.

Reflections with h+k+l=2n+1 are therefore *systematically absent*.

These statements apply equally well to x-ray and neutron diffraction and to powder as well as to single crystal diffraction data.

In the case of a powder sample, orientational averaging leads to a reduction of the dimensionality of the intensity information from 3D to 1D: Diffraction intensity I is recorded as a function $|\boldsymbol{\tau}| = 1/d_{hkl}$ or, by making use of Bragg's law, of $\sin(\theta)/\lambda$ or just as a function of 2θ. For powders, two additional corrections (M and P in eqn. 4.36) need to be applied in order to convert between the measured intensities I and the squared structure factor magnitudes F^2:

$$I(|\boldsymbol{\tau}|) = \text{SCALE} \cdot \text{L} \cdot \text{A} \cdot \text{E} \cdot \text{M} \cdot \text{P} \cdot |\boldsymbol{F}(|\boldsymbol{\tau}|)|^2 \qquad (4.36)$$

M is the multiplicity of the individual reflections and takes into account how many symmetrically equivalent sets of lattice planes correspond to a given hkl. In the cubic crystal system, for instance, $M_{111}=8$ (octahedron) while $M_{100}=6$ (cube). P is the so-called preferred orientation parameter which corrects the intensities for deviations from the assumption of randomly oriented crystals in the powder sample.

4.5 Diffractometers

Single Crystal Neutron Diffractometry

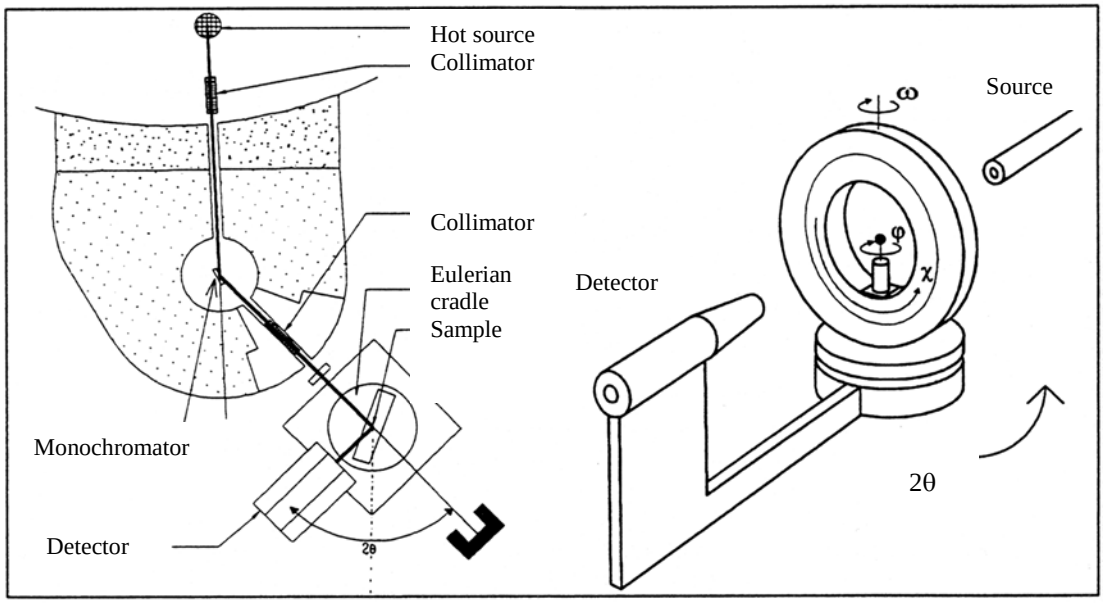

Fig. 4.18: *Principle components of a constant wavelength single crystal diffractometer.*

Monochromator and collimator

For constant wavelength diffraction, the energy (wavelength) and direction (collimation) of the incident neutron beam needs to be adjusted. For that purpose, the diffractometer is equipped with a crystal monochromator to select a particular wavelength band ($\lambda \pm \Delta\lambda/\lambda$) out of the "white" beam according to the Bragg condition for its scattering plane (*hkl)*

$$2d_{hkl} \cdot \sin\theta_{hkl} = \lambda, \qquad (4.37)$$

with the interplanar spacing d_{hkl} and the monochromator scattering angle $2\theta_{hkl} = 2\theta_M$. The width of the wavelengths band $\Delta\lambda/\lambda$, which is important for the Q-resolution,

depends on the divergences of the beam before and after the monochromator (collimations α_1 and α_2), on the mosaic spread of the monochromator crystal ΔM, and on the monochromator angle $2\theta_M$. In order to increase the intensity of the monochromatic beam at the sample position the monochromator crystal is often bent in vertical direction perpendicular to the diffraction plane of the experiment. In this way the vertical beam divergence is increased leading to a loss of resolution in reciprocal space. The diffracted intensity from the sample is measured as a function of the scattering angle 2θ and the sample orientation (especially in case of a single crystal). 2θ is again defined by collimators. As there is no analysis of the energy of the scattered beam behind the sample, the energy resolution $\Delta E/E$ of such a 2-axes diffractometer is not well defined (typically of the order of some %). In addition to the dominant elastic scattering also quasi-elastic and some inelastic scattering contributions are collected by the detector.

Neutron filters and the problem of λ/2 contamination

Unfortunately, the monochromator crystals not only "reflect" the desired wavelength λ by diffraction from the set of lattice planes (hkl) but also the higher orders of λ/2 or λ/3 etc. from 2h,2k,2l or 3h,3k,3l to the same diffraction angle:

$$\sin\theta=\lambda/d_{hkl} = (\lambda/2)/d_{2h\ 2k\ 2l} = (\lambda/3)/d_{3h\ 3k\ 3l} \qquad (4.38)$$

The only requirement is, that the higher order reflection (2h,2k,2l) or (3h,3k,3l) has a reasonably large structure factor (see chapter 4). Higher order contamination causes measurable reflection intensities at "forbidden" reflection positions and in addition to that can modify intensities at allowed positions. Thus it can very much affect the correct determination of the unit cell as well of the symmetry (from systematically absent reflections). The solution to this problem is to minimize the λ/2 contamination by using filters which suppress the higher orders stronger than the desired wavelength. One such type of filters uses resonance absorption effects - completely analogous to the suppression of the K_β line in x-ray diffractometers. Another way to attenuate short wavelengths is to use the scattering from materials like beryllium or graphite. These filters use the fact that there is no Bragg diffraction if $\lambda > 2d_{max}$, where d_{max} is the largest interplanar spacing of the unit cell. As we have shown above, for such long wavelengths the Ewald sphere is too small to be touched by any reciprocal lattice point. Below this critical wavelength, the neutron beam is attenuated by diffraction and this can be used to suppress higher order reflections very effectively. Frequently used materials are polycrystalline beryllium and graphite. Due to their unit cell dimensions, they are particularly suitable for experiments with cold neutrons because they block wavelengths smaller than about 3.5 A and 6 A respectively.

Resolution function:

An important characteristic of any diffractometer is its angular resolution. Fig. 4.19 shows (on the right) the resolution function (reflection half width as a function of scattering angle) for the four circle single crystal neutron diffractometer HEiDi at FRM II shown on the left. The resolution depends on a number of factors, among them the collimation, the monochromator type and quality, the 2θ and (hkl) of the reflection used for monochromatization etc.

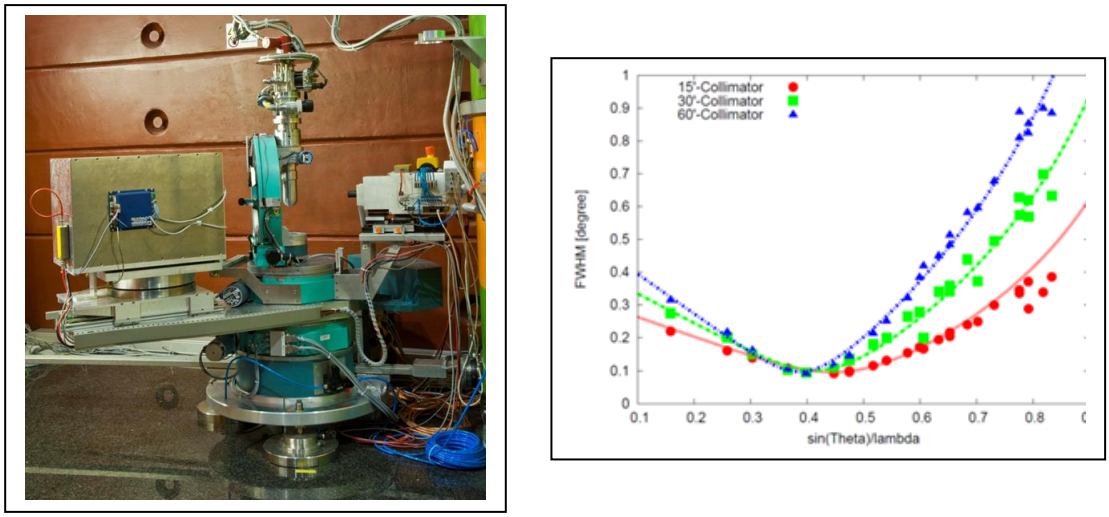

Fig. 4.19: *Left: Experimental setup of the four circle single crystal diffractometer HEiDi at FRM II. Right: Resolution function of HEiDi for different collimations, monochromator: Cu (220), 2ΘMono = 40° → λ = 0.873 Å.*

Powder Neutron Diffractometry:

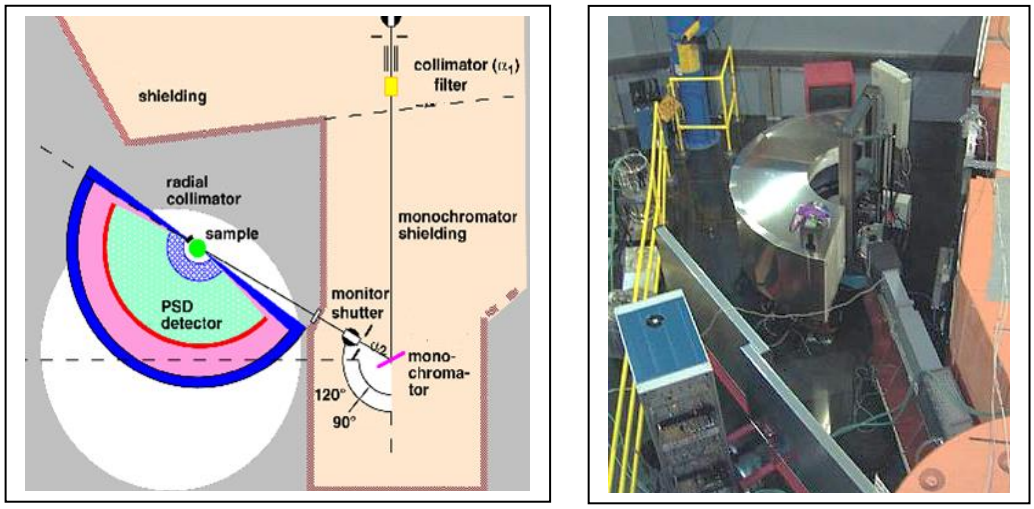

Fig. 4.20: *Left: Typical setup of a (constant wavelength) powder neutron diffractometer with position sensitive detector (PSD). Right: Neutron powder diffractometer SPODI at FRM II*

Neutron Rietveld analysis:

The conversion from 3D- to 1D-intensity data caused by the averaging over all crystallite orientations in a powder sample severely restricts the informative value of powder neutron (or x-ray) diffraction experiments and makes the resolution function of the instrument even more important than in the single crystal case. Even with optimized resolution, the severe overlap of reflections on the 2θ-axis often prohibits the extraction

of reliable integrated intensities from the experiment. Instead, the Rietveld method, also referred to as *full pattern refinement*, is used to refine a given structural model against powder diffraction data. The method, which is widely used in powder x-ray diffraction, has actually been invented by Hugo Rietveld in 1966 for the structural analysis from powder neutron data. Full pattern refinement means that along with the structural parameters (atomic coordinates, thermal displacements, site occupations) which are also optimized in a single crystal structure refinement, additional parameters like the shape and width of the reflection profiles and their 2θ-dependence, background parameters, lattice parameters etc. need to be refined.

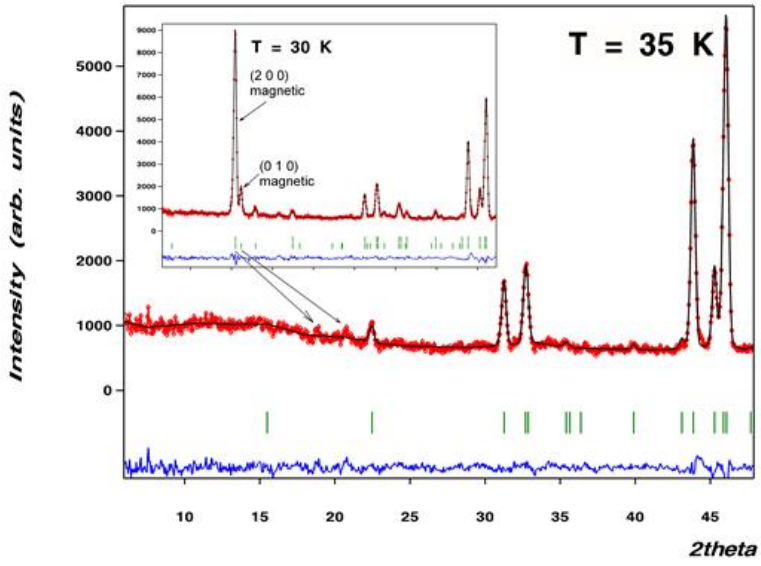

Fig. 4.21: *Results of a Rietveld refinement at the magnetic phase transition of $CoGeO_3$ [5], red: measured intensity, black: calculated from model, blue: difference, green: tick-marks at allowed reflection positions. The figure shows the low-angle part of two diffractograms measured at SPODI at 35K and 30K. Note the strong magnetic reflection appearing below the magnetic ordering transition (in the inset).*

References

[1] J. Strempfer et al. Eur. Phys. J B **14**, 63 – 72, (2000).
J. Strempfer et al. Physica B **267 - 268**, 56 – 59, (1999).
[2] A. Dianoux, G. Lander (Eds.) "Neutron Data Booklet",
Institute Laue-Langevin (2002)
[3] Reproduced from: Braggs world, talk by Th. Proffen
http://ebookbrowse.com/proffen-talk-bragg-pdf-d59740269
[4] Courtesy of Kevin Cowtan , http://www.ysbl.york.ac.uk/~cowtan/
[5] G. Redhammer et al. Phys. Chem. Min. **37**, 311-332, (2010) .

Exercises

E4.1 Types of Scattering Experiments

Discuss/define the following terms:

A. Elastic scattering, **B.** Inelastic scattering, **C.** Coherent scattering, **D.** Incoherent scattering

What is the major source of incoherent elastic scattering that is specific to neutrons?

E4.2 Energy and Wavelength

Give orders of magnitudes for the energy [eV] and the wavelength [Å] of the following types of radiation which are being used for diffraction experiments:

A. Thermal neutrons, **B.** x-ray photons, **C.** Electrons

E4.3 Scattering Length

Discuss the terms *(units, similarities, differences):*
A. Elastic scattering length, **B.** Elastic scattering cross section,
C. Atomic form factor (for x-rays)

E4.4 The Phase Problem

Describe, in simple terms, the "phase problem of crystallography"

A. Formulate the diffraction experiment in terms of the Fourier transform with subsequent squaring of the modulus of the Fourier coefficients

B. Discuss in how far these operations may be inverted.

C. Describe qualitatively how the phase problem is solved.

E4.5 Ewald Construction

Sketch the Ewald-construction for a single crystal experiment.

What is this geometric construction useful for?

E4.6 Intensity Corrections

The experimental Bragg-reflection intensity $I(\boldsymbol{\tau})$ and the squared modulus of the calculated structure factor $|\boldsymbol{F}(\boldsymbol{\tau})|^2$ (from the structure factor formula) are proportional to each other.

A number of corrections have to be made to get from $I(\tau)$ to $|\boldsymbol{F}(\tau)|^2$ or vice versa.

A. Recall *(from your experience with x-rays)* and discuss the physical origin of these intensity corrections:

SCALE: Scalefactor; L: Lorentz factor; A: Absorption correction, E: Extinction correction. For powder methods also: M: Multiplicity, P: Preferred orientation.

B. Discuss the relative importance of these factors for neutrons and x-rays.

C. The polarisation correction, which is important in x-ray scattering, is missing in the neutron case: Discuss this fact in terms of the different physical meaning of "polarization" for x-rays and neutrons.

E4.7 Fourier Transform

A. Define the terms "Fourier-analysis" and "Fourier-synthesis" in the context of a diffraction experiment *(formula and description)*

B. What is the purpose of calculating a Fourier synthesis in crystallography?

E4.8 Filtering

A. How does a beryllium filter work? What is it used for?

B. Discuss why filters are also used in laboratory x-ray diffraction.

E4.9 Systematic absences

Calculate (from the structure factor formula) the systematic absences of reflections for an orthorhombic C-centered lattice.